

From time to time, *Technical Soaring* will reprint significant papers from the past. These papers are still very relevant, but may have never been seen by some of our newer readers, or worth revisiting by those who enjoyed them when they originally appeared. Some of these classics have become hard to find, so we are glad to have the opportunity to make them available once again. This paper was originally published in *Technical Soaring*, Vol. 18, No. 3.

Critical Flutter Speed of Sailplanes Calculated for High Altitude: Examples of computation

Wojciech Celestyn Chajec

Presented at the XXIII OSTIV Congress, Borlänge, Sweden (1993)

Introduction

Flutter means the vibration of an aircraft or glider in flight caused by elastic, mass and aerodynamic forces. Only the aerodynamic forces - through the air density - are dependent upon the flight altitude. The flutter calculations determine the minimum flight speed, at which undamped vibrations may occur. This speed is named the critical flutter speed V_{CF} . In parallel, the frequency and mode shape of the vibration are determined.

The results presented here were obtained using the flutter calculation program founded by IPPT PAN in Warsaw (1) with some modification made in Mielec, for the prototypes (or their modifications) of the following Polish sailplanes, which are representative for particular classes:

- SZD-55 of standard class,
- SZD-56 "BB-1" of 15m-class with flaps,
- KR-03A, all-metal, two-seat training glider and
- PW-5, winner of the World Class competition.

The program determines the aerodynamic forces from Theodorsen's instationary aerodynamic theory. The results cover altitudes from 0 to 15,000m introducing the relation between air density and geopotential altitude H , practically equal to flight altitude, in accordance with ISO standard atmosphere. The V-g flutter calculation method was used, which was chosen for its speed (for one altitude the time of calculations is 1 minute on the 486-50MHz PC). This method gives at once critical speeds, frequencies and mode shapes of all flutter kinds; the critical flutter speed of each glider configuration is then the lowest flutter speed of the different flutter kinds.

On Fig. 1 is shown an example diagram V-g (the damping g , which should be added to the vibrating structure, in order to obtain harmonic motion, as a function of the flight speed V), for a particular flutter mode at an altitude $H=2000m$. To determine the critical speed of this flutter, the structural damping coefficient $g=0.02$ was assumed, for which undamped vibrations may occur over the speed range indicated. Above the V-g diagram is the H(V) diagram, which shows the flutter speed range for different altitudes. Change of altitude may also cause a change of frequency or mode shape.

Speed V on horizontal axis for both diagrams is an equivalent air speed (EAS), chosen rather than TAS because the diagrams are then simpler to interpret. In addition, if for determination of aerodynamic forces the quasi-stationary theory had been used, the calculated critical flutter speeds EAS

would be independent of altitude. For comparison, on almost all diagrams H(V), the chosen curve $TAS=const$ was drawn.

Variation of different kinds of flutter modes with altitude

Results for some modification of the PW-5 sailplane with free stick and loose rudder links (without pedal mass) are shown on the Fig. 2. The calculations are based on the theoretical mass and stiffness model corrected to comply with results of ground vibration tests. Structural modal damping coefficients were omitted. Global damping g equal to 0.03 was assumed. Capital letters refer to different flutter kinds, and where two frequencies are given, the first refers to $H = 0$ and the second to $H = 25$ km:

-symmetrical flutter modes:

B - wing bending/torsion + fuselage bending/elevator rotation with frequency of 15 Hz and 11 Hz;

C - wing bending/torsion - fuselage bending/elevator rotation with frequency of 9 and 8 Hz (minus means motion in opposite direction);

-antisymmetrical flutter modes:

V - horizontal fuselage and wing bending/rudder rotation with frequency of 5 Hz;

L - fundamental wing bending/aileron rotation with frequency of 11 and 6 Hz;

N - fuselage antisymmetrical bending (and stabilizer rotation)/rudder rotation with frequency of 12 Hz;

U - second harmonic wing bending and torsion/aileron rotation with frequency of 14 and 15 Hz.

The fig. is interesting, because it contains probably all typical kinds of V_{CF} variation with altitude:

- small dependency of V_{CF} from altitude (e.g. B and C flutter modes),

- great dependency of V_{CF} from altitude (L flutter mode),

- flutter at high altitudes only (V flutter mode).

V flutter appears only over 3000m altitude and can be eliminated by slight increasing of rudder mass balance.

Fig. 3 contains the flutter calculation results of the prototype of SZD-55 glider based on measured vibration modes, frequencies and modal damping coefficients. The modes were orthogonalised with theoretical mass model use. This fig. shows the example without water ballast with stick and pedals free. In this case, the V_{NE} is limited

by two flutter modes:

B - symmetrical wing and fuselage bending flutter with elevator rotation and frequency of 11 Hz,

L - antisymmetrical wing bending / aileron rotation flutter with frequency 4 and 6 Hz.

Examination of the H(V) diagrams shows the conclusions described below.

The typical diagram for control surface flutter is similar to a parabola, see Fig. 1. Dr F. Kiessling noted, that the line connecting the points for which the motion is least damped (or most divergent), usually is close to line $EAS = \text{const}$. The change of the critical speed with flight altitude depends not only on this line but also on the parabola width. For aileron flutter (mode L) and for symmetric wing flutter with aileron rotation or torsion (mode E) it is typical to have a very wide curve H versus V. In the case of flutter caused by rudder rotation (mode V) the width is usually small.

In the example shown in Fig. 1, the apex line of flutter E is slightly out of plumb tilted to higher speeds at higher altitudes. In spite of that, the big spread of the parabola's arms results in a strong decrease in the critical speed, at some point even more than corresponds to $TAS = \text{const}$.

Variation of critical flutter speed (EAS) of other flutter kinds with altitude is not significant. It is presented in Fig. 2, flutter C and Fig. 4, flutter S.

Calculation of the critical speed of control surface flutter

The examples shown indicate that the critical speed of control surfaces flutter varies strongly with altitude. Of course, these kinds of flutter may usually be eliminated by increasing mass balance of the control surface sufficiently. However, full (statical or only dynamical) mass balance of control surfaces may reduce the performance of the glider, so it should be optimal. Flutter elimination through the increase of structural stiffness is better, but may increase the glider mass and/or cost. Considering the above, it is important, to use correct design, having regard to the possibility of appearance of backlash, friction or other nonlinearities in the control system. In addition, the control system elements have their mass and elasticity. Much information on this subject was gathered in (6), and the method of considering nonlinearities using harmonic linearization was shown in (3).

The necessity for consideration of control system element masses in flutter calculations, and a simple way of doing so, was described in (8). Thanks to the consideration of elevator control system elements mass, it was possible to explain and eliminate symmetrical flutter (Fig. 4,5) which was discovered in SZD-56 prototype flight tests with water ballast in the front tanks (Spring, 1991).

The classical methods of mode determination are based on a simplified theoretical model of rudder, elevator, aileron and flaps. In this model, named "spring-mounted control surface" model, the control surface is assumed to be attached to the stabilizer, fin or wing by means of hinges and a hinge-moment counterbalancing spring. The pushrods, levers or links

connecting the control surface with stick, pedal or control lever are ignored. However, experience showed that in modern gliders with light control surfaces, this model is inadequate; the control system elements mass need to be considered in full.

Fig. 6 shows the configuration of the SZD-56 glider elevator control system in the fin. The arrows indicate the selected, elementary displacements utilized in the theoretical model used for calculations of vibration.

In this case control system elements were grouped as follows: one group contained those that only increase the elevator deflection energy and having no effect upon any couplings of the elevator deflection with other elementary displacements of the glider, while the others included those control system elements which - like pushrods 1 or 2 and anti-flutter mass 3 - cause such couplings.

As far as the first group of elements is concerned, it was assumed that the energy of that portion of their motion which is identical to the motion of the particular element of the glider's structure, has been accounted for in the "spring-mounted elevator" model. Any additional displacement due to elevator deflection are orthogonal to the displacements accounted for in that model. In case of, for example, pushrod 4 this assumption is satisfied because elevator deflection results in the pushrod's displacement along the fuselage longitudinal axis, and the computational model ignores the fuselage displacements in this direction. The kinetic energy of elevator control system elements was represented by additional terms of mass matrix.

Considering the elements included in the other group, one must account for their whole kinetic energy induced by the glider motion. In the example (Fig. 6), there is consideration of the energy of elements 1, 2 and 3 resulting from the rotation and displacement of the vertical tail, as well as from displacements and angles of rotation appropriate to the stabilizer center section and the elevator.

The results of calculation done this way are presented in Fig. 4 and they pertain to the SZD-56 glider with 2 x 80 kg water ballast in the front tanks. The calculation was based on the theoretical mass and stiffness model corrected to obtain compliance with result of a ground vibration test. The measured modal damping factors were taken into consideration. The following flutter modes are drawn:

E - symmetrical bending flutter of the wing's tips with aileron rotation and frequency about 25 Hz, typical for a glider with water ballast in the wing.

S - torsional flutter of fin with rudder rotation and fuselage bending, with frequency about 11 Hz,

B - symmetrical fuselage bending flutter with elevator rotation, with frequency of 9 Hz.

Flutter B almost precisely corresponds to the vibration found during flight at indicated airspeed close to 150 km/h. The mode shape of this type of flutter is illustrated in Fig. 5.

Calculations showed that mass 3 has a favorable effect. This was confirmed in flight, no B flutter occurring

with mass 3 installed.

Another mode of flutter of frequency 30Hz and low amplitude, was recorded in flight probably elevator rotation within backlash range. This was eliminated by adding small mass balances on the elevator tips.

Conclusions

The calculations of this investigation showed that critical flutter speed EAS goes down as altitude increases. In case of control surface flutter the decrease may exceed 5km/h for each thousand meters of altitude, and in exceptional cases may be similar to the decrease designated by $TAS = \text{const}$. There are also some kinds of flutter which are possible at high altitude only. As the result of this situation, if the critical flutter mode is not known, there is no basis for altering the existing reduction is; V_{NE} over 3000m (or over the test flight altitude) according to the law $TAS = \text{const}$.

However one should realize that the situation shown for example in Fig. 1 does not often occur. Usually V_{CF} decreases more slowly with altitude increase. Also the limits in some cases could be set by two (Fig. 3) or even more kinds of flutter. Hence, the possibility of changing the regulations should be considered for well documented cases. The V_{NEF} speed at altitudes higher than H_F - flutter test altitude - could have been described as $K_F V_{CF}$, where K_F is equal to V_{NE} / V_{CF} at H_F , as in reference (7).

Because of the possibility of the appearance of new instability areas at altitudes exceeding the test flight altitude, it is recommended that the flutter analysis should be extended up to the estimated operational ceiling of the sailplanes before test flights are started.

The wider flutter analysis would involve just slightly higher cost of calculations. The most time consuming part of the calculations is the creation of the calculation model and the determination of proper vibrations is already done. To obtain the results for different flight altitude, a change of only one parameter (air density) and a little extra computer work is required.

References

- (1) M. Nowak, W. Potkanski, "Metodyka analizy flatteru samolotów lekkich" (in Polish, *Flutter Analysis of Light Aeroplanes*) Prace Instytutu Lotnictwa, nr 65, Warszawa 1976.
- (2) W. Chajec, W. Potkanski, "Flutter Analysis of Gliders", XIX OSTIV Congress, Rieti, OSTIV Publication XVIII, 79-83, 1985.
- (3) W. Potkanski, *Flutter Analysis of Light Aircraft*, Acta Mechanica 62, 105-112, Springer Verlag, 1986.
- (4) W. Potkanski, W. Chajec, "Flutter Analysis During the Design of Airplane", *Technical Soaring*, Vol. XIII No.4, 135-140, 1989.
- (5) F. Kiessling, "On Simplified Analytical Flutter Clearance Procedures for Light Aircraft", DLR-FB 89-56, Goettingen 1989.
- (6) W. Stender, F. Kiessling, "Aeroelastic Flutter Prevention in Gliders and Small Aircraft", DLR-Mitt. 91-03, Goettingen 1991.
- (7) F. G. Irving "The Influence of Flutter Consideration on the Never-exceed Speed", OSTIV Sailplane Development Panel, 1991.
- (8) W. Chajec, "Uwzględnianie mas elementów układu sterowania w obliczeniach flatteru" (in Polish, *Accounting for Airplane Control System Elements Mass in Flutter Calculations*), Prace Instytutu Lotnictwa nr132, Warszawa 1993.

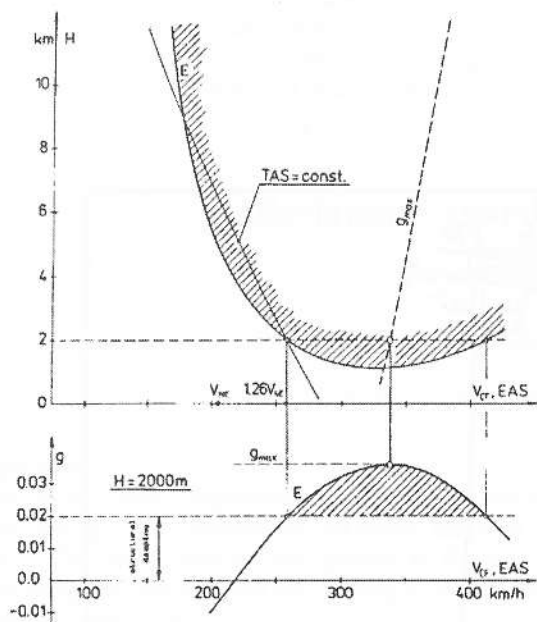


Figure 1. Variation of critical speed of symmetrical wing torsion flutter E with rotation and torsion ailerons, with frequency of about 19 Hz. This calculation was made for KR-03A sailplane with reduced torsion ailerons stiffness.

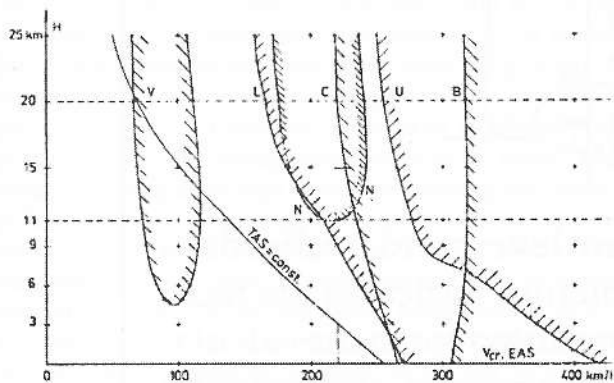


Figure 2. The flutter calculation results of sample modification of PW-5 sailplane.

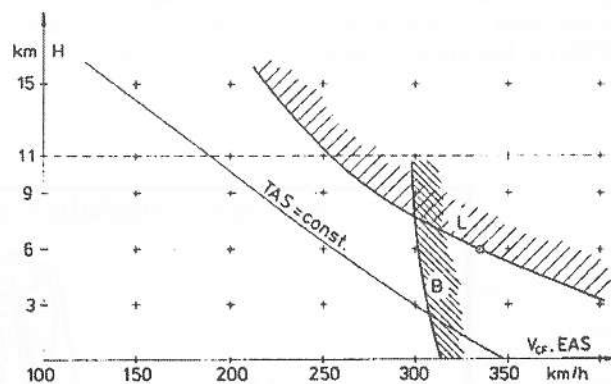


Figure 3. Variation of calculated V_{CF} with altitude for SZD-55 prototype with both the control stick and pedals free.

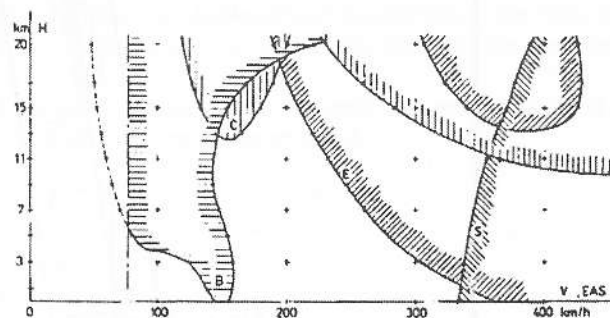


Figure 4. Results of flutter calculation for prototype of SZD-56 glider before the anti-flutter mass balance.

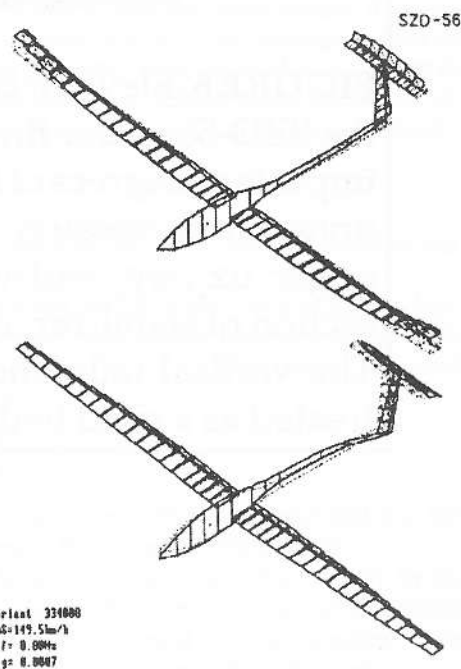


Figure 5. Mode shape of flutter B from calculation shown on Fig. 4 for flight at sea level.

